

Effects of Simultaneous Operation on the Biograph mMR

Sebastian Fürst¹, Isabel Dregely¹, Stephan Nekolla¹, Markus Schwaiger¹, and Sibylle Ziegler¹
¹Department of Nuclear Medicine, Technische Universität München, Munich, Bavaria, Germany

Introduction:

The advent of combined positron emission tomography (PET) and computed tomography (CT) scanners in the clinical environment in the early 2000s and their immediate success have significantly increased interest in other multimodal imaging systems and accelerated their development, with PET and MR being in the centre of the efforts. Their integration, however, was far more challenging than the one of PET and CT, mainly because conventional PET photodetectors cannot be operated in magnetic fields. Moreover, the fast switching of gradients and the transmission of RF pulses interfere with standard PET front-end electronics and vice versa, whereas the presence of PET detectors affects magnetic-field homogeneity. Previous studies already showed that with the release of the first integrated whole-body PET/MR machine, these challenges were overcome without sacrificing performance compared to stand-alone PET and MR scanners [1]. The impact of simultaneous operation on the measured properties was also found to be negligible for this system. The aim of the present work was to investigate the effects of MR sequences on PET data acquisition further and in more detail, focusing on energy spectra and count rates.

Materials and Methods:

For the purpose of this study, a set of measurements was carried out on the Biograph mMR (Siemens, Erlangen, Germany). This integrated PET/MR machine is based on a clinical MR scanner with a 3T magnet (length: 163cm, bore diameter: 60cm), a gradient coil system (length: 159cm, amplitude: 45mT/m, slew rate: 200T/m/s) and a RF body coil (peak power: 35kW, transmitter bandwidth: 800kHz). The PET detectors are integrated into the system and located between the gradient and the body coils. The PET component contains 8 rings with 56 detector blocks (ring diameter: 65.6cm, axial FOV: 25.8cm). Each detector block consists of 8 x 8 LSO crystals (4 x 4 x 20mm³) read out by an array of 3 x 3 avalanche photodiodes (APD), which serve as photodetectors. Cooling channels, pre-amplifiers and other front-end electronics are integrated into the detector blocks as well. The energy resolution is 14.5% (measured with Ge68 in air) and the window of accepted energies 430-610keV. A method for temperature compensation is implemented as well. For all measurements, a cylindrical Ge68 phantom (radius: 10cm, length: ~37cm, activity: 39MBq) was placed on the patient table and moved to the centre of the FOV, aligned with the scanner axis. In the first three experiments, crystal energy spectra were acquired for 2min. Then, Dixon (3D acquisition, TR/TE: 3.6ms/1.23ms, FOV: 450 x 349mm², voxel size: 3.7 x 2.3 x 2.7mm³, 128 partitions, flip angle: 10.0°, TA: 19s), UTE (TR/TE: 11.94ms/0.07ms, FOV: 300 x 300mm², voxel size: 1.6 x 1.6 x 1.6mm³, 192 partitions, flip angle: 10.0°, TA: 100s) or TrueFISP (3D acquisition, TR/TE: 7.83ms/3.92ms, FOV read/phase: 180mm/100%, 0.7mm slice thickness, in-plane resolution: 0.5 x 0.5mm², 64 partitions, flip angle: 57.0°, TA: 306s) sequences were repeatedly run for 15min. After that, energy spectra were again recorded in the same manner, but with the respective sequences running. Temperatures were logged every 30s using sensors installed in circuit boards adjacent to the detector cassettes. In a fourth measurement, PET count rates were studied over 30min. At first, data were acquired without MR sequences. After 5min, the Dixon sequence was started, 12min after the beginning of the measurement the UTE and 11min prior to the end of the measurement the TrueFISP 3D sequences.

Results:

The measured temperature changes near the detector cassettes range between 1.6°C and 11.9°C, 2.1°C and 2.9°C and between 0.9°C and 3.6°C for the Dixon, UTE and TrueFISP sequences, respectively. A slight broadening of the photo peak in the energy spectra and a shift to lower energy channels reflect temperature increases in the APD, albeit less strong. Moreover, the overall number of events in the spectra increased, when the MR was running, with the strongest growth in the lower-energy Compton region compared to the photo peak. In the plot of PET trues count rate against time, the intervals with the MR working can be clearly identified. For all three sequences, the count rate first drops by ~0.5%. It then recovers and exceeds the one without MR by ~0.8%, before falling to the original level again. The run of the curve depends on the particular sequence. The effect is least pronounced in the case of the Dixon sequence.

Conclusion:

As was already reported for the BrainPET insert [2], simultaneously applied MR sequences may affect PET count rates in the case of the Biograph mMR as well. In contrast to [2], in this study not only decreases, but also increases in count rates were observed, pointing towards competing mechanisms in the detectors or the electronics. However, it is safe to neglect these effects in the clinical practice due to their small scale.

Acknowledgments:

Deutsche Forschungsgemeinschaft (DFG), Graduate School of Information Science in Health (GSISH)/TUM Graduate School

References:

- [1] Delso G et al., *Journal of Nuclear Medicine*, in press
- [2] Weirich C et al., *Proceedings of the Annual Meeting of the ISMRM 2011*

Figure 2. Plot of trues count rate against time. 5min, 12min and 19min after the start of the PET acquisition, standard clinical Dixon, UTE and TrueFISP 3D sequences were run.

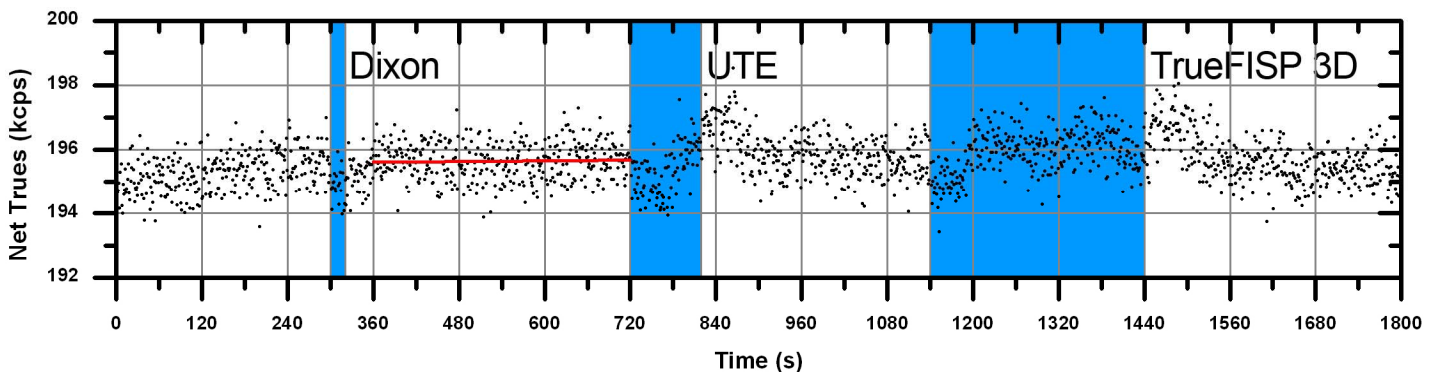


Figure 1. Energy spectra before (bottom) and after (top) 15min of running a UTE sequence.

